Available online at www.sciencedirect.com
ScienceDirect
Mathematics and Computers in Simulation 82 (2012) 1102–1111
MATHEMATICS AND COMPUTERS IN SIMULATION
www.elsevier.com/locate/matcom

Euler characteristics of oceanic sea states

Francesco Fedele [a,*], Guillermo Gallego [b], Anthony Yezzi [b], Alvise Benetazzo [c], Luigi Cavaleri [c], Mauro Sclavo [c], Mauro Bastianini [c]

[a] *School of Civil and Environmental Engineering, Georgia Institute of Technology, Atlanta, USA*
[b] *School of Electrical & Computer Engineering, Georgia Institute of Technology, Atlanta, USA*
[c] *ISMAR-CNR, Venice, Italy*

Received 17 November 2009; received in revised form 26 April 2011; accepted 16 May 2011
Available online 26 May 2011

Abstract

We present an application of a novel Variational Wave Acquisition Stereo System (VWASS) for the estimation of the wave surface height of oceanic sea states. Specifically, we show that VWASS video technology combined with statistical techniques based on Euler Characteristics of random fields provides a new paradigm for the prediction of wave extremes expected over a given area of the ocean.

Keywords: Euler characteristics; Oceanic waves; Image processing; Partial differential equations; Stereo epipolar; Variational methods

1. Introduction

The prediction of large waves is typically based on the statistical analysis of time series of the wave surface displacement retrieved from wave gauges, ultrasonic instruments or buoys at a fixed point P of the ocean. However, in short-crested seas the surface time series gathered at the given location tends to underestimate the true actual wave surface maximum that can occur over a given region of area S around P. Indeed, large waves travel on top of wave groups, and the probability that the group passes at its apex through P is practically null. The large crest height recorded in time at P is simply due to the dynamical effects of a wave group that focuses nearby that location within or outside S forming a larger wave crest. Thus, point measurements can underestimate the global maximum $\eta_{\max}$ of the wave surface height η attained over S. Only in narrow-band sea states, point measurements are exact in predicting such maximum which is expected to be the same at any point in space. However, realistic oceanic conditions are generally short-crested and the expected $\eta_{\max}$ can be underestimated if wave extremes are not modeled both in space and time as maxima of random fields rather than those of random processes of time [1,17,3]. The predictions of such space-time extremes rely on the exceedance probability

$$\Pr\left\{\max_{P\in S}\eta(P) > h\right\} \tag{1}$$

* Corresponding author.
E-mail address: ffedele3@gtsav.gatech.edu (F. Fedele).

0378-4754/$36.00 © 2011 IMACS. Published by Elsevier B.V. All rights reserved.
doi:10.1016/j.matcom.2011.05.009

of the global maximum of η over S. For Gaussian fields, asymptotic solutions of (1) are given by Piterbarg [17], and by Adler [1] and Adler & Taylor [3] exploiting Euler Characteristics (*EC*) of random excursion sets. The application of such advanced stochastic theories to realistic oceanic conditions requires the availability of wave surface data measurements collected in space on the scale of few hundred meters or smaller. At such scales, the main difficulty for such measurements is that radar or SAR remote sensing is not accurate enough to reconstruct the space-time dynamics and associated spectral properties. On the other hand, a two dimensional wave probe-type array could be used but it can be expensive to install and maintain.

In this paper, we overcome these limitations by proposing to use Euler Characteristics techniques in combination with video observational technologies to predict wave extremes over a given area. Specifically, we propose a novel Variational Wave Acquisition Stereo System (VWASS) able to acquire four-dimensional (4D) video data (both in space and time) of oceanic states. Indeed, the rich statistical content of 4D data allows reliable estimates of the expected largest wave surface height over an area via Euler Characteristics' theory [1,3]. VWASS has a significant advantage as a low-cost system in both installation and maintenance. Further, it provides spatial and temporal data whose statistical content is richer than that of a time series retrieved from a buoy, which is expensive to install and maintain. VWASS exploits the combination of state-of-the-art epipolar methods (Benetazzo [4]) and variational partial differential equation techniques (Gallego et al. [12]) for the 4D stereo reconstruction of the spatio-temporal dynamics of ocean waves.

The paper is structured as follows. We first briefly review the theory behind the variational VWASS and then introduce the *EC* of excursion sets of random fields. We then estimate the *EC* of spatial snapshots of oceanic sea states acquired via VWASS and the associated exceedance probability (1). The broader impact of these results to oceanic applications is finally discussed.

1.1. The stereo variational geometric method

The reconstruction of the wave surface from stereo pairs of ocean wave images is a classical problem in computer vision commonly known as the correspondence problem (Ma et al. [16]). For VWASS we solve this by two distinct approaches based on epipolar geometries and variational techniques. In the former, the 'epipolar algorithm' of Benetazzo [4] finds corresponding points in the two images, from which the estimate of the real point in the three dimensional terrestrial coordinate system can be obtained. However, this approach may fail to provide a smooth surface reconstruction because of 'holes' associated to unmatched image regions [4,16]. This is typical during cloudy days, when at a given point on the water surface the same amount of light is received from all possible directions and reflected towards the observer causing a visual blurring of the specularities of the water. In this case, the water surface is said to support a Lambertian radiance function [16]. Variational techniques overcome this problem. Under the assumptions of a Lambertian surface, following the seminal work by Faugeras and Keriven [7], the three dimensional (3D) reconstruction of the water surface at a given instant in time is obtained in the context of active surfaces by evolving an initial surface through a PDE derived from the gradient descent flow of a cost functional designed for the stereo reconstruction problem.

To be more specific, the energy being maximized is the normalized cross correlation between the image intensities obtained by projecting the same water surface patch onto both image planes of the cameras. It is clear that such energy depends on the shape of the water surface. Therefore, the active surface establishes an evolving correspondence between the pixels in both images. Hence, the correspondence will be obtained by evolving a surface in 3D instead of just performing image-to-image intensity comparisons without an explicit 3D model of the target surface being reconstructed.

To infer the shape of the water surface $\eta(x, y)$ at the location (x, y) over an area S, we set up a cost functional on the discrepancy between the projection of the model surface and the image measurements. As previously announced, such cost is based on a cross correlation measure between image intensities, which will be noted as $E_{\text{data}}(\eta)$. We conjecture that, to have a well-posed problem, a regularization term that imposes a geometric prior must also be included, $E_{\text{geom}}(\eta)$. We consider the cost functional to be the (weighted) sum:

$$E(\eta) = E_{\text{data}}(\eta) + E_{\text{geom}}(\eta). \tag{2}$$

In particular, the geometric term favors surfaces of least area:

$$E_{\text{geom}}(\eta) = \int_{\eta} dA. \tag{3}$$

The data fidelity term may be expressed as:

$$E_{\text{data}}(\eta) = \int_{\eta} \left(1 - \frac{\langle I_1, I_2\rangle}{|I_1| \cdot |I_2|}\right) dA, \tag{4}$$

where η is the wave surface region within the field of views of both cameras, and $\langle I_1, I_2\rangle$ is the cross-correlation between the image intensities I_1 and I_2.

The surface η is found by minimizing E via a gradient flow-based iterative algorithm that starts from an initial estimate of the surface at time $t=0$, η_0, and it will make the surface evolve towards a minimizer of E, hopefully converging to the desired water surface shape. Given a function $\Phi : \Re^3 x \Re^3 \to \Re^+$ ($\Re^3$ and $\Re^+$ are the 3D Eucledian space and that of real positive numbers, respectively) and the energy

$$E = \int_{\eta} \Phi(X, N)\, dA \tag{5}$$

with N as the unit normal to η at X, a theorem in Faugeras and Keriven [7] says that the flow that minimizes E is given by the evolution PDE

$$\eta_t = \beta N, \tag{6}$$

where η_t is the derivative of η with respect to a fictitious time variable, and the speed β in the normal direction to the surface that drives the evolution is:

$$\beta = 2H(\Phi - \Phi_N \cdot N) - \Phi_X \cdot N - \text{trace}\left[(\Phi_{XN})_{T_\eta} + dN \circ (\Phi_{NN})_{T_\eta}\right]. \tag{7}$$

All quantities are evaluated at the point $\eta = X$ with normal N to the surface. H denotes the mean curvature. Φ_X, Φ_N are the first-order derivatives of Φ, while Φ_{XN}, Φ_{NN} are the second-order derivatives. dN is the differential of the Gauss map of the surface and $(\cdot)_{T_\eta}$ means "restriction to the tangent plane T_η to the surface at $\eta = X''$. Note that our proposed energy (2) can be expressed in the form of (5) if $\Phi = (1 - \langle I_1, I_2\rangle / |I_1| \cdot |I_2|) + \alpha$, where α is just a weight for the geometric prior. In practice, we use the flow based on the first-order derivatives of Φ because it provides similar results to those of the complete expression, but saves a significant amount of computations,

$$\eta_t = (2H(\Phi - \Phi_N \cdot N - \Phi_X \cdot N))N. \tag{8}$$

The level set framework has been adopted to numerically implement (8) by Gallego et al. [12]. We have tested the variational reconstruction algorithm using a set of images, shown in the upper panel of Fig. 1, acquired by Benetazzo [4] on a water depth of 8 meters. In the lower panel of the same figure it is shown the successful reconstructed surface. Hereafter, we introduce the concept of Euler characteristics that will be applied to predict the expected number of large maxima in oceanic sea states exploiting the high statistical content of the acquired video data via VWASS. The stereo algorithm can then be applied sequentially to reconstruct the evolution of the wave surface in time.

1.2. Euler characteristics

In algebraic topology, the Euler characteristic EC is classically defined for polyhedra according to the formula:

$$EC = V - E + F, \tag{9}$$

where V, E, and F are respectively the numbers of vertices, edges and faces in the given polyhedron. The same definition given in (9) can be adapted to two dimensional (2D) sets which are the focus of this paper. In this case, the EC is also equivalent to the difference between the number connected components (CC) and holes (H) of the given set, viz.

$$EC = CC - H. \tag{10}$$

For a generic 2D set Σ with complicated regions, computing the EC from the definition (10) presents some challenges. A computationally efficient approach can be devised based on (9). Following Adler [1] we first define a Cartesian mesh

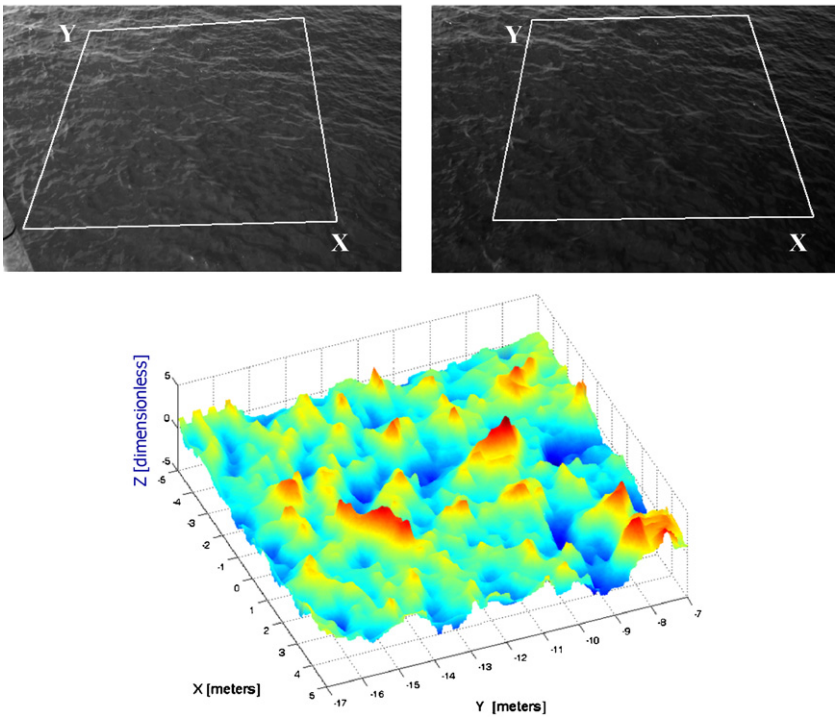

Fig. 1. (Upper panel) input stereo pair images to the algorithm. The rectangular domain (8 m × 8.7 m) of the reconstructed surface has been superimposed. The wave height is in the range ±0.2 m. (Lower panel) reconstructed normalized wave surface η via VWASS.

grid Γ of size $(\Delta x, \Delta y)$ that approximates the complicated domain of the given set Σ. The $EC(\Gamma)$ is then computed as follows. Denote F as the number of squares (faces) composing Γ, E_h (E_v) as the number of horizontal (vertical) segments between two neighboring mesh points and V the number of grid points. The $EC(\Gamma)$ then follows from (9) setting $E = E_h + E_v$. As the grid cell size $\Delta x \Delta y$ tends to zero, $EC(\Gamma) \to EC(\Sigma)$. For example, for a square, according to (9), $EC = 4\text{-}4 + 1 = 1$ and this is in agreement with (10) since there is only 1 connected component and no holes.

Consider now a 2D random field η as a model for oceanic sea states. At a given instant of time, a snapshot of η over a given region S is shown in Fig. 2. The excursion set

$$U_{\eta,h} = \{(x, y) \in S : \eta(x, y) > h\}$$

is the portion of the region S where η is above the threshold h. From Fig. 2 it is clear that the EC of an excursion set depends very strongly on h. If this is low, then EC counts the number of holes in the given set. If the threshold is high (see Fig. 2, right panel), then all the holes tend to disappear and the EC counts the number of connected components, or local maxima of the random field. If η is Gaussian and stationary, an exact formula for the expected value of EC, valid for any threshold, was discovered by Adler [1] and Adler and Taylor [3] in the explicit form

$$\overline{EC(U_{\eta,h})} = N_S \xi \exp\left(-\frac{\xi^2}{2}\right), \tag{11}$$

where $\overline{(\bullet)}$ means expectation, $\xi = h/\sigma$ is a normalized threshold amplitude, σ is the standard deviation of η and

$$N_S = A_S (2\pi)^{-3/2} \sigma^{-2} |\Lambda|^{1/2} \tag{12}$$

is the number of 'waves' over the area A_S of S, with Λ as the covariance matrix of the gradient $\nabla\eta$. For small S, the excursion set can touch the boundary of S and correction terms need to be added [20].

We point out that the EC of random excursion sets is relevant to oceanic applications because of the work by Adler [1] and Adler and Taylor [3]. Indeed, they have shown that the probability that the global maximum of η exceeds a threshold h is well approximated by the expected EC of the excursion set $U_{\eta,h}$, provided the threshold is high. Indeed, as h increases the holes in the excursion set $U_{\eta,h}$ disappear until each of its connected components includes just one

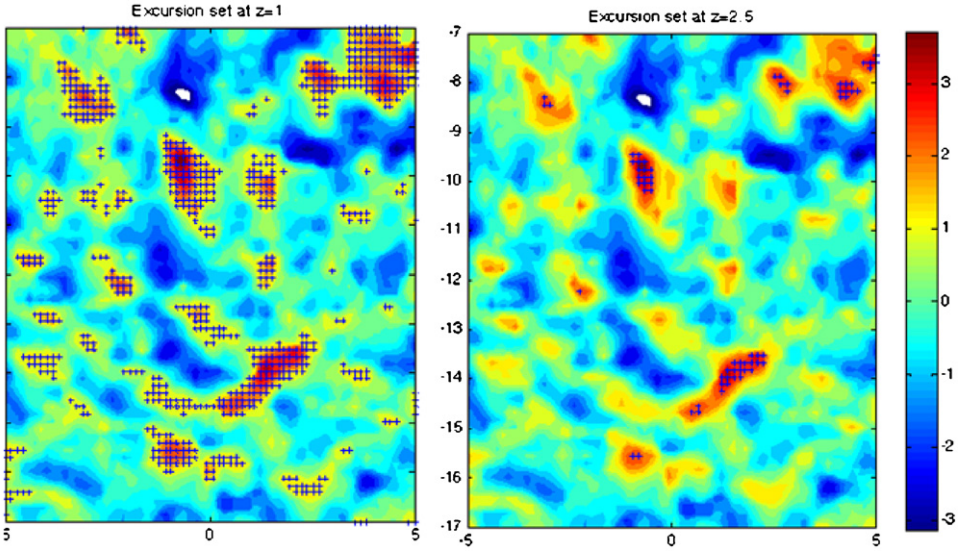

Fig. 2. Excursion sets (cross points) of a normalized zero-mean Gaussian field Z at the threshold $z=1$ (left) and $z=2.5$ (right), respectively. Note that, as the threshold increases the excursion set is the union of isolated regions delimiting the local maxima of Z.

local maximum. Thus, the *EC* counts the number of local maxima as shown in the right panel of Fig. 2. For very large thresholds, the *EC* equals 1 if the global maximum exceeds the threshold and 0 if it is below. Thus, heuristically the $EC(U_{\eta,h})$ of large excursion sets is a binary random variable with states 0 and 1, and for $h>>\sigma$,

$$Pr\left\{\max_{P\in S}\eta(P)>h\right\}=\Pr\left\{EC(U_{\eta,h})=1\right\}=\overline{EC(U_{\eta,h})}. \tag{13}$$

Note that the global maximum of η is the largest wave surface height expected over the area S. Thus, (13) provides the basis for the estimate of exceedance probabilities of large wave surface amplitudes by means of the *EC* of excursion sets of video images retrieved via VWASS (see Fig. 1).

At first glance, that the *EC* relates to global maxima may appear odd. In reality there is a deep connection between the two. Indeed, Adler [1] proved that the expected number $EX_{\max}$ of large local maxima greater than h equals the expected *EC* of large excursion sets, viz.

$$EX_{\max}(h)\approx\overline{EC(U_{\eta,h})},\quad \text{for } h>>\sigma. \tag{14}$$

This statement can be readily proved following the heuristic argument below. For a very large threshold h, the excursion set $U_{\eta,h}$ of a Gaussian field $\eta(x,y)$ is the union of disjoint elliptical regions covered by local maxima above h, as shown in Fig. 3. We can thus apply the Poisson clumping heuristics of Aldous [2] as follows.

Without losing generality, consider η Gaussian on a Cartesian coordinate system (t,s) so that the covariance matrix Λ of $\nabla\eta$ is diagonal with spectral moments m_{tt} and m_{ss} ($m_{tt}>m_{ss}$) and the determinant $|\Lambda|=m_{tt}m_{ss}$. Note that t, s are the principal directions of η and the partial derivatives $\partial_t\eta$ and $\partial_s\eta$ are thus uncorrelated and stochastically independent. Now, define $EX_{lm}(z)dz$ as the number of local maxima with amplitude in $[z, z+dz]$ so that the expected number $EX_{\max}(h)$ of maxima larger than h follows as

$$EX_{\max}(h)=\int_h^\infty EX_{lm}(z)dz. \tag{15}$$

Further, on the plane $\eta=h$ define the area $\Gamma(z,h)$ of the footprint of a local maximum with amplitude $z>h$ (see Fig. 3). The wave surface around this maximum that occurs at, say, $t=t_0$ and $s=s_0$, is described by the conditional Slepian model [1,5,13–15]

$$\eta_c=\{\eta(t,s)\,|\eta(t_0,s_0)=z\}=\frac{z}{\sigma^2}\Psi(t-t_0,s-s_0)+R, \tag{16}$$

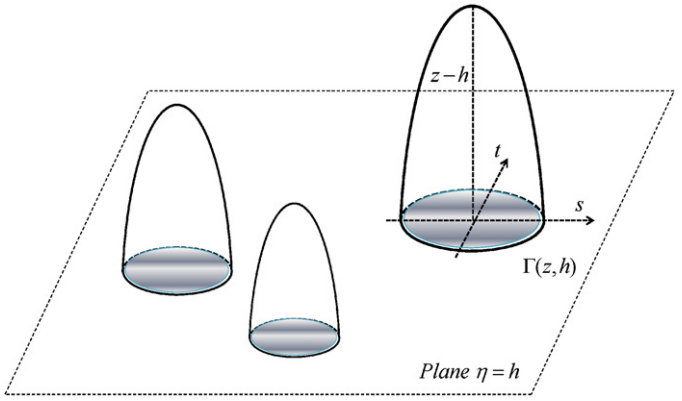

Fig. 3. A typical excursion set $U_{\eta,h}$ of a Gaussian field $\eta(x,y)$, above a very large threshold h. The set is the union of disjoint elliptical regions covered by the local maxima above h. $\Gamma(z,h)$ denotes the area of the elliptical footprint.

where Ψ is the covariance of η and R is a random residual of $O(z^0)$. For $z>>1$, R can be neglected and Taylor-expanding (16) nearby $t=t_0$ and $s=s_0$ yields

$$\eta_c = z - z\left(\frac{m_{tt}}{2\sigma^2}(t-t_0)^2 + \frac{m_{ss}}{2\sigma^2}(s-s_0)^2 + \ldots\right), \tag{17}$$

where $m_{tt}=\partial_{tt}\Psi$, $m_{ss}=\partial_{ss}\Psi$ are evaluated at (t_0,s_0). By setting $\eta_c=h$, $\Gamma(z,h)$ follows from (17) as the area of the ellipse of equation $(t-t_0)^2/a^2+(s-s_0)^2/b^2=1$ with semi-axises $a=\sigma\sqrt{2\,(z/h-1)\,/m_{tt}}$ and $b=\sigma\sqrt{2\,(z/h-1)\,/m_{ss}}$, that is

$$\Gamma(z,h) = \pi\, ab = \frac{2\pi\sigma^2}{\sqrt{m_{tt}m_{ss}}}\frac{z-h}{h} = \frac{2\pi\sigma^2}{\sqrt{|\Lambda|}}\frac{z-h}{h}. \tag{18}$$

From Fig. 3, on the plane $\eta=h$ the excursion set $U_{\eta,h}$ is the union of disjoint elliptical footprints of the local maxima above large threshold h, and from (18) its area is given by:

$$A_{\rm m}(h) = \int_h^\infty EX_{lm}(z)\Gamma(z,h)dz = \frac{2\pi\sigma^2}{\sqrt{|\Lambda|}}\int_h^\infty EX_{lm}(z)\frac{z-h}{h}dz, \quad \text{for } h>>\sigma. \tag{19}$$

On the other hand, at any threshold h, the area of the excursion set $U_{\eta,h}$ is given by:

$$A(\eta\geq h) = A_S\int_h^\infty p(\eta=w)dw, \tag{20}$$

where the probability density function (pdf) $p(\eta)$ is Gaussian. Thus, for $h>>\sigma$ we must have $A(\eta\geq h)=A_{\rm m}(h)$ and (19) and (20) lead to the following Volterra integral equation of first kind

$$\int_h^\infty p(\eta=w)dw = \frac{2\pi\sigma^2}{A_S\sqrt{|\Lambda|}}\int_h^\infty EX_{lm}(z)\frac{z-h}{h}dz, \quad \text{for } h>>\sigma, \tag{21}$$

for the unknown $EX_{lm}(z)$. The solution of (21) proceeds by differentiating both members of (21) twice with respect to h, and setting $h=z$. This yield, for $z>>\sigma$,

$$EX_{lm}(z) = A_S(2\pi)^{-3/2}\sigma^{-2}|\Lambda|^{1/2}\left(\frac{z}{\sigma}\right)^2\exp\left(-\frac{z^2}{2\sigma^2}\right). \tag{22}$$

Using (22), the asymptotic leading term in (15), after integration by parts, is given by:

$$EX_{\max}(h) \cong A_S(2\pi)^{-3/2}\sigma^{-2}|\Lambda|^{1/2}\frac{h}{\sigma}\exp\left(-\frac{h^2}{2\sigma^2}\right), \quad \text{for } h >> \sigma, \tag{23}$$

which is identical to $\overline{EC(U_{\eta,h})}$ of (11) if we set $\xi = h/\sigma$.

2. Oceanic sea states

We extend (11) to deal with the expected *EC* of excursion sets of spatial snapshots of oceanic sea states measured by VWASS (see Fig. 1). To properly model oceanic nonlinearities we follow Tayfun [18] and define the dimensionless nonlinear wave surface ζ_{nl} over S as:

$$\zeta_{nl} = \zeta + \frac{\mu}{2}(\zeta^2 - \hat{\zeta}^2), \tag{24}$$

where $\zeta = \eta/\sigma$, $\hat{\zeta}$ is the Hilbert transform of ζ, and $\mu = \lambda_3/3$ is the wave steepness which relates to the skewness λ_3 of ζ_{nl}. We note that other nonlinear processes similar to (24), such as those in Cao [6], could be used to model ocean waves as well. Hereafter, we adopt the Tayfun model (24) since it is physically based [18] and it has been proved to accurately model wave extremes [8,9,19].

For $\xi >> 1$, the excursion regions, where $\zeta_{nl} \geq \xi$, include just isolated local maxima. So, the structure of the excursion set can be related to the surface field locally to a maximum of ζ_{nl} with amplitude greater or equal to ξ. Assume that this occurs at $t = t_0$ and $s = s_0$. Then, the surface locally around that maximum is described by the nonlinear Slepian model defined by the conditional process [8,9,19]

$$\zeta_{nc} = \{\zeta_{nl}(t,s)\,|\zeta_{nl}(t_0,s_0) \geq \xi\}. \tag{25}$$

Unfortunately, this does not have a straightforward explicit solution. Nonetheless, a simplification of (25) stems from the particular structure of the nonlinear surface ζ_{nl} as follows. Note that, from (24) it is clear that the nonlinear quadratic component of ζ_{nl} is phase-coupled to the extremes of the Gaussian ζ. So, a large maximum of ζ_{nl} greater or equal to ξ occurs simultaneously when ζ itself is at a large maximum with an amplitude greater or equal to, say, ξ_1. Thus, for $\xi_1 >> 1$, the conditional process (24) is equivalent to the simpler process [8,9]

$$\zeta_{nc} = \{\zeta_{nl}(t,s)\,|\zeta(t_0,s_0) \geq \xi_1\} = \xi_1\Psi + \frac{\mu}{2}\xi_1^2(\Psi^2 - \hat{\Psi}^2), \tag{26}$$

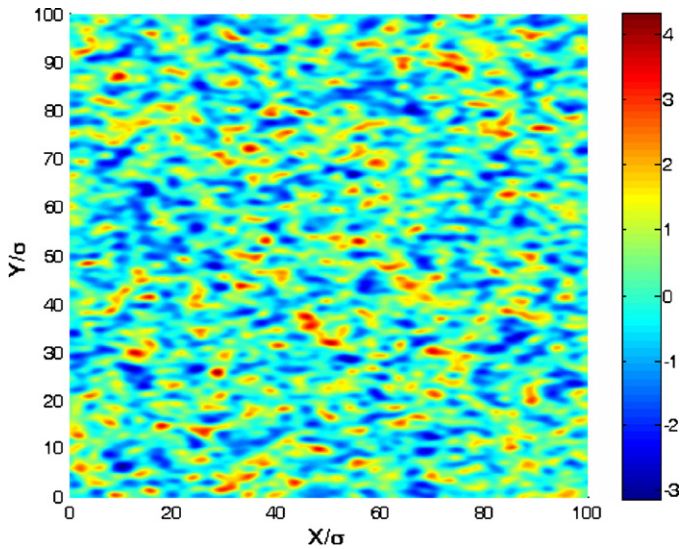

Fig. 4. Realization of the broadband nonlinear field ζ_{nl}/σ (linear spectrum is Gaussian, $\mu = 0.1$).

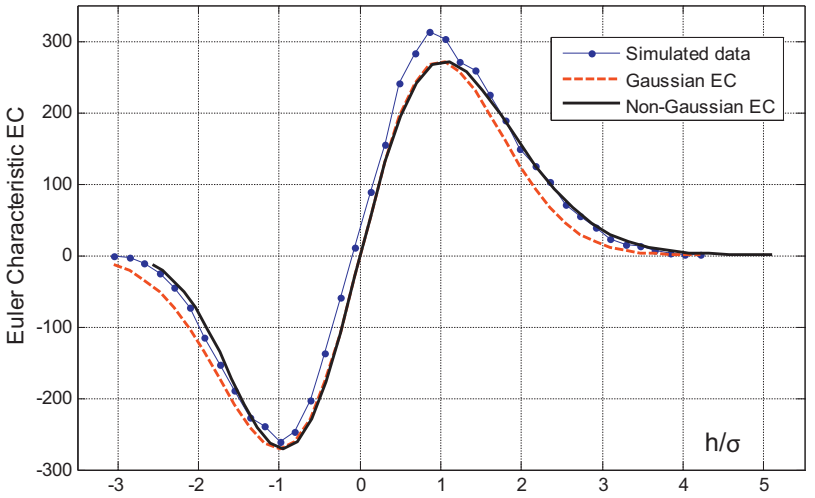

Fig. 5. Observed *EC* from the simulated field of Fig. 4 and the expected *EC* against the threshold h.

where Ψ is the covariance of ζ. From (26), the nonlinear crest occurs at $t=t_0$ and $s=s_0$, where $\Psi=1$ and $\hat{\Psi}=0$, and its amplitude is given by:

$$\xi = \xi_1 + \frac{\mu}{2}\xi_1^2. \tag{27}$$

Thus, the expected *EC* of the excursion set $\{\zeta_{nl} \geq \xi\}$ equals that of the *EC* of the excursion set $\{\zeta \geq \xi_1\}$ of the Gaussian ζ. By the variable transformation (27), from (11) it follows that

$$\overline{EC(U_{\zeta_{nl},\xi})} = N_S \frac{-1+\sqrt{(-1+2\mu\xi}}{\mu} \exp\left[-\frac{(-1+\sqrt{(-1+2\mu\xi})^2}{2\mu^2}\right]. \tag{28}$$

Fig. 4 shows a particular realization of a broadband nonlinear ζ_{nl} simulated using (24) over an area $A_S=100^2\sigma^2$ covering roughly $N=436$ waves ($\mu=0.1$). Further, Fig. 5 plots the observed *EC* against the threshold h. In the same

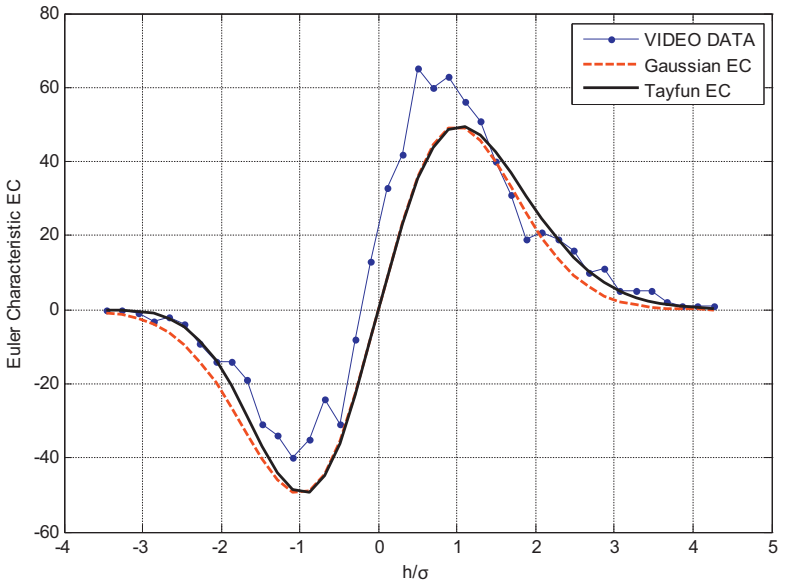

Fig. 6. Observed and expected *EC*s against the threshold h, as for the oceanic video data collected via VWASS of Fig. 1.

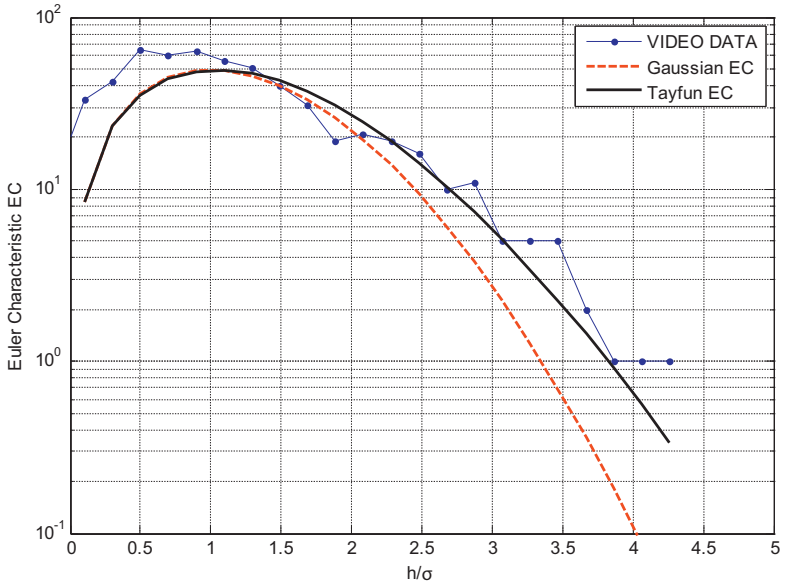

Fig. 7. Same as in Fig. 6: observed and expected *EC*s over the positive range of the threshold h.

figure, the expected nonlinear Tayfun *EC* in (28) is compared against that Gaussian (11). The simulated data agree well with the Tayfun model over the extremes whereas the Gaussian *EC* underestimates data for larger thresholds as expected.

Consider now the VWASS reconstruction of the oceanic sea state shown in Fig. 1. The observed *EC* of the estimated wave surface is plotted in Fig. 6 against the threshold h. For comparison, the expected theoretical *EC*s for the linear and nonlinear case are also plotted. Clearly, the experimental data also fairly match the Tayfun *EC* model (28) over the extremes (see also Fig. 7).

3. Conclusions

We have presented an application of a novel variational image sensor VWASS for the stereo reconstruction of wave surfaces. VWASS has a significant advantage as a low-cost system in both installation and maintenance. Further, it provides spatial and temporal data whose statistical content is richer than that of a time series retrieved from a buoy, which is expensive to install and maintain. We believe that the proposed statistical analysis of oceanic sea states based on Euler Characteristics is essential for a proper design of coastal and offshore structures. Indeed, Forristall [10] used such theoretical results to explain the damages sometimes observed on the lower decks of platforms after storms [11]. These may be due to a design that underestimates the largest crest height expected over the area nearby the offshore structure. Thus, VWASS is a promising video technology that, combined with statistical tools based on Euler Characteristics, provides reliable estimates of wave extremes over a given oceanic area.

Acknowledgments

The authors would like to acknowledge Hailin Jin for providing source code that was partly used to obtain the results shown in this paper. Alvise Benetazzo is also grateful to Professor Ken Melville and Luc Lenain, of the Scripps Institution of Oceanography (SIO), San Diego, for the support received. We also thank Harald Krogstad for useful discussions and suggestions.

References

[1] R.J. Adler, The Geometry of Random Fields, John Wiley, NY, 1981.
[2] D. Aldous, Probability Approximations via the Poisson Clumping Heuristic, Springer-Verlag, NY, 1989.

[3] R.J. Adler, J.E. Taylor, Random Fields and Geometry, Springer, NY, 2007.
[4] A. Benetazzo, Measurements of short water waves using stereo matched image Sequences, Coastal Engineering 53 (2006) 1013–1032.
[5] P. Boccotti, Wave Mechanics for Ocean Engineering, Elsevier Science, Oxford, 2000.
[6] J. Cao, The size of the connected components of excursion sets of χ^2, t and F Fields, Adv. Appl. Probab. 31 (3) (1999) 579–595.
[7] O. Faugeras, R. Keriven, Variational principles, surface evolution, pde's, level set methods and the stereo problem, IEEE Trans. Image Process. 7 (3) (1998) 336–344.
[8] F. Fedele, Rogue waves in oceanic turbulence, Physica D 237 (14–17) (2008) 2127–2131.
[9] F. Fedele, M.A. Tayfun, On nonlinear wave groups and crest statistics, J. Fluid Mech. 620 (2009) 221–239.
[10] G.Z. Forristall, Maximum wave heights over an area and the air gap problem, in: Proc. ASME 25th Inter. Conf. Off. Mech. Arc. Eng., Hamburg, OMAE2006-92022, 2006, pp. 11–15.
[11] G.Z. Forristall, Wave crest heights and deck damage in hurricanes Ivan, Katrina and Rita, Proc. Offshore Technology Conference, Houston, USA, OTC 18620, 2007.
[12] G. Gallego, A. Benetazzo, A. Yezzi, F. Fedele, Wave spectra and statistics via a variational wave acquisition stereo system, in: Proc. ASME 27th Inter. Conf. Off. Mech. Arc. Eng., Estoril, Portugal, OMAE2008-57160, 2008, pp. 801–808.
[13] M. Kac, D. Slepian, Large excursions of gaussian processes, Ann. Math. Statist. 30 (1959) 1215–1228.
[14] G. Lindgren, Some properties of a normal process near a local maximum, Ann. Math. Statist. 4 (6) (1970) 1870–1883.
[15] G. Lindgren, Local maxima of gaussian fields, Ark. fur Mat. 10 (1972) 195–218.
[16] Y. Ma, S. Soatto, J. Kosecka, S. Shankar Sastry, An Invitation to 3-D Vision: From Images to Geometric Models, Springer-Verlag, NY, 2004.
[17] V. Piterbarg, Asymptotic Methods in the Theory of Gaussian Processes and Fields, American Mathematical Society, 1995.
[18] M.A. Tayfun, On narrow-band representation of ocean waves. Part I. Theory, J. Geophys. Res. 1 (C6) (1986) 7743–7752.
[19] M.A. Tayfun, F. Fedele, Expected shape of extreme waves in sea storms, 26th ASME Int. Conf. Offshore Mechanics and Arctic Eng., San Diego, USA, OMAE2007-29073, 2007, pp. 53–60.
[20] K.J. Worsley, Boundary corrections for the expected Euler characteristic of excursion sets of random fields, with an application to astrophysics, Adv. App. Prob. 27 (1995) 943–959.